*optics*

**MDPI**

*Article*

# Introducing Optical Nonlinearity in PDMS Using Organic Solvent Swelling

**Sudhakara Reddy Bongu** [1,2], **Maximilian Buchmüller** [1,2], **Daniel Neumaier** [2] **and Patrick Görrn** [1,2,*]

1    Chair of Large Area Optoelectronics, University of Wuppertal, Rainer-Gruenter-Str. 21,
     42119 Wuppertal, Germany; bongu@uni-wuppertal.de (S.R.B.); buchmueller@uni-wuppertal.de (M.B.)
2    Wuppertal Center for Smart Materials and Systems, University of Wuppertal, Rainer-Gruenter-Str. 21,
     42119 Wuppertal, Germany; dneumaier@uni-wuppertal.de
*    Correspondence: goerrn@uni-wuppertal.de

**Abstract:** The feasibility of introducing optical nonlinearity in poly-dimethyl siloxane (PDMS) using organic solvent swelling was investigated. The third-order nonlinear refraction and absorption properties of the individual materials, as well as the PDMS/solvent compounds after swelling were characterized. The well-established Z-scan technique served as characterization method for the nonlinear properties under picosecond pulsed laser excitation at a 532 nm wavelength. These experiments included investigations on the organic solvents nitrobenzene, 2,6-lutidine, and toluene, which showed inherent optical nonlinearity. We showed that nitrobenzene, one of the most well-known nonlinear optical materials, has proven suboptimal in this context due to its limited swelling effect in PDMS and comparatively high (non)linear absorption, resulting in undesirable thermal effects and potential photo-induced damage in the composite material. Toluene and 2,6-lutidine not only exhibited lower absorption compared to nitrobenzene but also show a more pronounced swelling effect in PDMS. The incorporation of toluene caused a weight change of up to 116% of PDMS, resulting in substantial nonlinear optical effects, reflected in the nonlinear refractive index of the PDMS/toluene composite $n_2 = 3.1 \times 10^{-15}$ cm$^2$/W.

**Keywords:** transparent Kerr materials; self-focusing; poly-dimethyl siloxane; swelling; nonlinear solvents

## 1. Introduction

Nonlinear optical (NLO) effects play a crucial role in a variety of applications, including ultra-fast laser technology, telecommunications, and nonlinear imaging [1–5]. Historically, inorganic crystals, such as lithium niobate (LiNbO$_3$) or beta barium borate (BBO), have been widely used as NLO materials due to their strong nonlinearities over a broad range of optical frequencies [2]. However, integrating such crystals into photonic systems can be challenging because of their mechanical fragility, complex fabrication conditions, and their lack of scalability [6,7]. Semiconductors such as GaN and GaAs, which are well-established in optoelectronic applications like light-emitting diodes, also manifest nonlinear optical effects [8–11]. Over the past decade, a diverse set of promising alternatives has emerged within the field of NLO materials. These alternatives include polymers [12], as well as metal-halide perovskites [13], and two-dimensional (2D) materials [14,15], offering a more facile and scalable way of fabrication using solution-based methods at room temperature. To achieve high efficiency of the nonlinear interaction of these materials with light, it has become common practice to enhance the electromagnetic field locally using resonances supported by nanostructures. For the fabrication of such nanostructures on large areas, bottom-up methods like block-copolymer self-assembly [16,17] and the alignment of nanoparticles from suspension [18,19] or through wet-chemical synthesis [20,21] have emerged as promising approaches, which harness the self-alignment of structural elements.

Although resonances can enhance nonlinear optical effects, the increased light–matter interaction comes at a cost—it limits the operation bandwidth [22]. Resonant optical phenomena occur only at particular frequencies, resulting in a reduced ability to uniformly enhance the broadband NLO response of many materials. In addition, this selectivity may hinder transparency, making it crucial to find a balance between enhanced light–matter interaction and operation bandwidth. Especially, for applications where light must propagate over long distances through the optical device, highly transparent and scalable NLO materials are desperately sought today. For instance, such applications include optical waveguide structures, in which light propagation properties can be controlled using slight variations in the refractive index of at least one of the waveguide layers [23,24]. Various organic solvents, notably carbon disulfide ($CS_2$), nitrobenzene ($C_6H_5NO_2$), as well as toluene ($C_7H_8$) and acetone ($C_3H_6O$), exhibit promising nonlinear optical properties and often possess considerable transparency [25]. However, handling liquids in optical systems is often technologically challenging.

In this article, we present a method to facilitate the integration of nonlinear organic solvents into optical device architectures based on solid films. The approach involves incorporating organic solvents into poly-dimethyl siloxane (PDMS), through a process known as swelling, which has been used in microfluidic devices and lab-on-a-chip systems [26,27]. PDMS is a versatile and widely used silicon-based organic polymer. Renowned for its optical transparency, flexibility, and ease of fabrication; PDMS has become a material of choice in a variety of applications including optical devices such as waveguides or lenses, as well as stretchable electronics [28,29]. In photonics, PDMS has proven its applicability particularly for stretchable optical components, modulators, and sensors [30]. The inherent biocompatibility of PDMS further extends its utility in biological and medical applications. In the scope of incorporating optical nonlinearity into PDMS, various approaches have been reported in the literature. Some methodologies involve the integration of nonlinearity through the introduction of chromophores [31,32], plasmonic nanoparticles [33,34], perovskites [35,36], and 2D materials [37,38] into the PDMS. However, a prevalent challenge associated with these techniques is the simultaneous introduction of absorption, particularly noticeable in the case of dyes. Notably, the absorption of light can limit the applicability of these materials, especially in optical waveguide with high propagation lengths. The method presented in this paper addresses this concern, as it allows for the integration of nonlinearity into PDMS while preserving its transparency. Swelling of PDMS with organic solvents refers to the phenomenon where liquids diffuse into the PDMS matrix and alter its structure, leading to an increase in volume. When PDMS comes into contact with certain organic solvent, it undergoes such a swelling process, while the degree of swelling depends on factors such as the specific solvent used, time of exposure, and the inherent compatibility between PDMS and the solvent [39]. The primary objective of our paper is to facilitate the integration of transparent organic solvents with strong optical nonlinearity into optical devices. Recognizing the potential of these solvents in nonlinear optics, we seek to overcome challenges associated with their liquid nature by embedding them within a solid polymer host matrix.

## 2. Materials and Methods

A two-component silicone elastomer (Mavom Sylgard 184) consisting of a precursor component and a curing agent was used for preparing the PDMS films. The two components were mixed at a ratio of 10:1 and were manually stirred. De-airing was carried out in a vacuum chamber for 30 min. The optically transparent mixture was then cast into a Teflon mould (30 mm × 30 mm) up to the desired film thickness. A glass slide at the bottom of the Teflon mould ensured the formation of a smooth interface to minimize light scattering in the optical experiments. The PDMS was then cured at 80 °C for 60 min. The obtained film was cut into four samples of equal size The film thicknesses have been measured without contact, using an optical microscope. The focus of the microscope was subsequently aligned to the lower and upper boundary of the film and the height difference

of the objects has been measured. In the optical measurements, one sample was used as a reference, the other samples were used for further processing. To incorporate organic solvents into the PDMS host matrix, the PDMS samples were immersed in three different solvents: nitrobenzene (NB), 2,6-lutidine (LT), and toluene (TL). After a swelling time of 3 h, the samples were removed from the solvent baths and the swelling was quantified by measuring the weight change of the samples before and after swelling. For the optical measurements, the samples were fixed between two quartz slides using a Teflon frame (see insets in Figure 1) and then encapsulated using a chemical-resistant glue to prevent solvent evaporation.
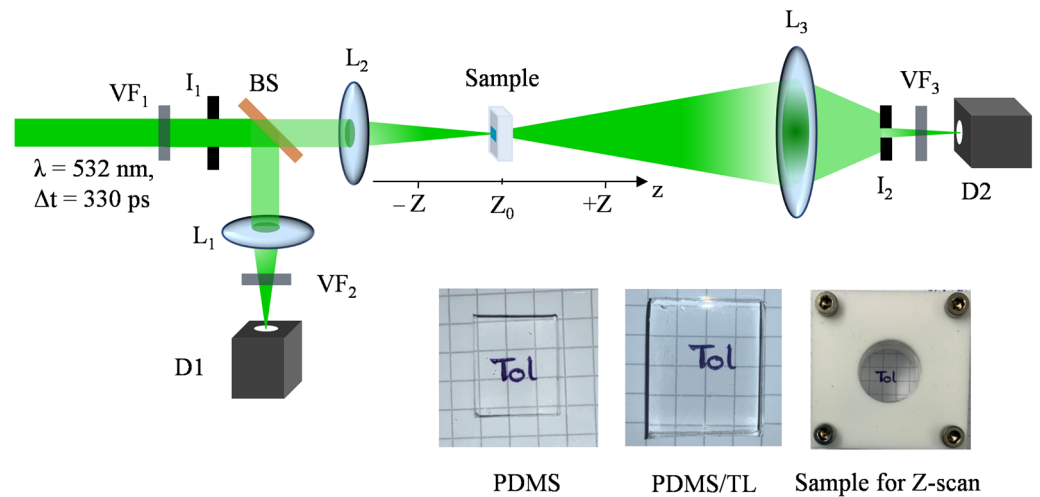


**Figure 1.** Scheme of the sample-preparation process and the layout of the Z-scan setup.

For characterizing the nonlinear optical properties of the samples we used the well-established Z-scan technique [40,41]. Figure 1 further shows the layout of the optical setup, which was used in our experiments. A pulsed solid-state laser (frequency-doubled Nd:YAG, Teem Photonics, Meylan, France) with a pulse width of 330 ps and a wavelength of 532 nm was used as an excitation source. Firstly, a variable neutral density filter (VF) and a variable iris ($I_1$) are used to adjust the optical power and the beam size of the laser beam. The optical power was monitored using a beam splitter (BS) and photodetector $D_1$. The main beam then passes through a biconvex lens ($L_2$, $f = 20$ cm) and is focused to a position $Z_0$. The transmitted light was collected using an additional lens ($L_3$, $f = 15$ cm). The variable iris $I_2$ enables the performance of both open-aperture (OA) as well as closed-aperture (CA) Z-scan measurements within the same beam path. The linear transmittance of the iris $I_2$ was set to $S = 1$ and $S = 0.4$ for OA and CA Z-scan measurements, respectively. Photodiode power sensors (S151C, Thorlabs, Bergkirchen, Germany) were used as photodetectors $D_1$ and $D_2$. For the measurements, the sample was moved along the $z$-direction using a linear stage and a stepper motor.

The nonlinear optical indices of the samples were determined by fitting the experimental data with the theoretical model. By considering a Gaussian beam excitation in the low irradiance limit (small beam distortion) the normalized transmittance in a CA Z-scan measurement for thick samples (sample thickness $L > z_R$) is given using

$$T(z) = 1 + \Delta\varnothing F(x,l),\tag{1}$$

where $F(x,l) = \dfrac{1}{4}\ln\left(\dfrac{\left[\left(x+\frac{l}{2}\right)^2+1\right]\left[\left(x-\frac{l}{2}\right)^2+9\right]}{\left[\left(x-\frac{l}{2}\right)^2+1\right]\left[\left(x+\frac{l}{2}\right)^2+9\right]}\right).\tag{2}$

Here, $x = \frac{z}{z_R}$ and $l = \frac{L}{z_R}$, where $L$ is the sample thickness, $z_R \left(= \frac{\pi \omega_0^2}{\lambda}\right)$ is the Rayleigh length with $\omega_0$, and $\lambda$ are the beam waist radius at the focal plane focus and the vacuum wavelength, respectively. $\Delta\varnothing = n_2 k_0 I_0 L_{eff}$ is the on-axis phase shift caused by nonlinear refraction. Here, $n_2$ is the third-order nonlinear refractive index, $k_0 = \frac{2\pi}{\lambda}$ the wave vector, $I_0$ the irradiance, and $L_{eff} = \frac{1 - \exp(-\alpha L)}{\alpha}$ is the effective path length, with $\alpha$ being the linear absorption coefficient. If the sample is sufficiently thin ($L \leq z_R$), Equation (1) converges to the following thin sample approximation:

$$T(z) = 1 + \frac{4x\Delta\varnothing}{(x^2 + 1)(x^2 + 9)} \tag{3}$$

Furthermore, we derived the real part of the third-order nonlinear susceptibility $\text{Re}\left(\chi^{(3)}\right)$ using the following equation [2]:

$$\text{Re}\left(\chi^{(3)}\right) = \frac{4}{3}n_0^2 \varepsilon_0 c n_2 \tag{4}$$

Here, $n_0$ is the linear refractive index, $\varepsilon_0$ is the electric constant, and $c$ is the vacuum speed of light. For the composite materials, a weighted mean of the refractive index was calculated according to the mass ratios.

## 3. Results

In the first step, we investigated the nonlinear optical properties of pure PDMS as well as various organic solvents using OA and CA Z-scan measurements at a pulse energy of 5.6 µJ and a pulse repetition rate of 50 Hz. The results are shown in Figure 2 and indicate a distinct nonlinear optical behaviour in different organic solvents. All solvents exhibit a valley-peak profile, which corresponds to self-focusing (positive values for $n_2$) and originates from the optical Kerr effect. In NB, we observed the strongest Kerr effect among all three candidates. Utilizing the parameters of the fitting curve (depicted as red curve in Figure 2a), we quantified the Kerr effect in NB with a nonlinear refractive index of $n_2 = 22 \times 10^{-15}$ cm$^2$/W. Additionally, we observed two-photon absorption (2PA) in NB, as shown in the inset of Figure 2a displaying the results of an OA Z-scan measurement. Also in the case of LT and TL, Kerr nonlinearity was observed (see Figure 2b,c), although it was less pronounced than in nitrobenzene. The nonlinear refractive indices of both LT and TL were found to be $n_2 = 7.1 \times 10^{-15}$ cm$^2$/W (approximately three-times smaller than for NB). Multiphoton absorption effects were not observed in LT and TL. In addition, pure PDMS did not show any detectable nonlinearity at a pulse energy of 5.6 µJ (Figure 2d). The results presented in Figure 2 highlight the solvent-specific nonlinear optical responses, with nitrobenzene demonstrating the most significant effect; this is, however, accompanied by nonlinear absorption, which can lead to parasitic thermal contributions to nonlinearity under increased irradiance which is discussed later in this paper.

In the next step, we evaluate the feasibility of introducing Kerr nonlinearity to the PDMS using solvent swelling. Therefore, PDMS films were immersed into the three different organic solvents. Depending on the solvent, the swelling of the PDMS happens on different time scales, and different amounts of the solvents can be incorporated. Figure 3 illustrates the solvent-specific swelling behaviour of PDMS depending on the exposure time. At the stage of saturated swelling, the thicknesses of the samples (initially 3 mm in all cases) were found to be 3.1 mm (NB), 3.3 mm (LT), and 4 mm (TL). Thus, NB stands out as the solvent with the least swelling effect among the three candidates, inducing a mere 5.4% weight change in PDMS. On the other hand, LT shows a stronger effect, causing around 36.5% weight alteration. Notably, TL emerges as the strongest candidate, generating a substantial 116.3% weight change. Thus, despite NB exhibiting a stronger Kerr effect, the data shown in Figure 3 reveal a significant limitation in the ability of NB to generate

swelling in PDMS. In contrast, Toluene, with an intrinsic nonlinearity only three times less than NB, facilitates an incorporation into PDMS that is more than 20 times higher.
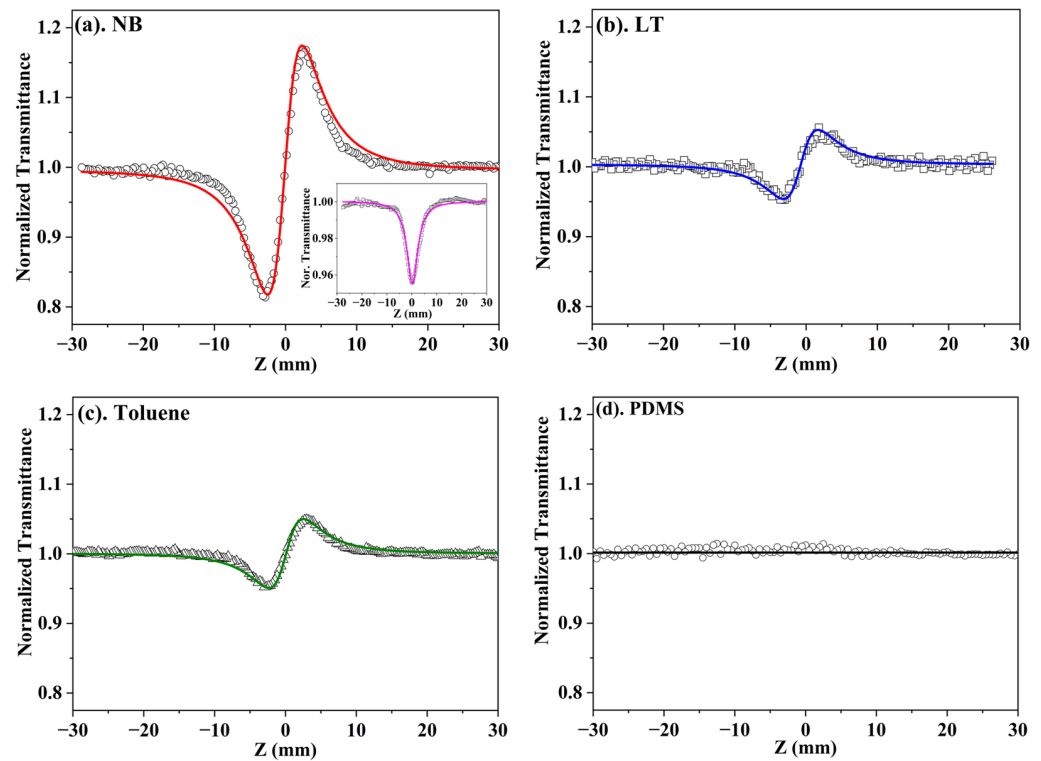


**Figure 2.** Closed aperture Z-scan profiles of nonlinear solvents and the PDMS film. Symbols are the experimental data and solid lines indicate the theoretical fit.
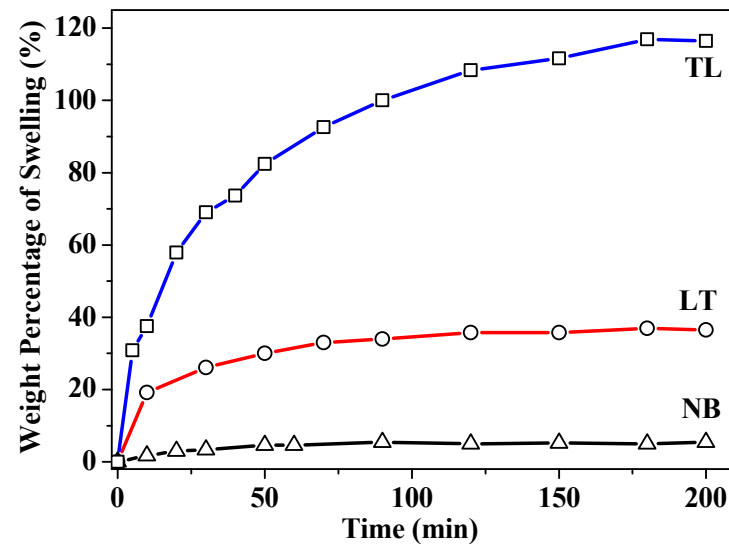


**Figure 3.** Measured weight change of the PDMS samples over time due to solvent swelling.

In Figure 4, the closed aperture Z-scan profiles of the PDMS-TL and PDMS-LT samples at 532 nm, measured with a pulse energy of 5.4 µJ are shown. Both samples show a self-focusing behaviour like in the pure solvents. Compared to the PDMS-LT, PDMS-TL exhibits a twice-stronger effect of third-order nonlinear refraction (see Figure 4) with a nonlinear refractive index of $n_2 = 3.1 \times 10^{-15}$ cm$^2$/W. The OA scan measurements confirm the absence of any nonlinear absorption processes for PDMS/TL and PDMS/LT. In contrast, PDMS/NB shows a strong thermally induced nonlinear optical response for

identical experimental conditions. This thermal effect results from linear absorption and two-photon absorption (2PA) of NB at a 532 nm wavelength, which leads to the generation of local heat. In fact, the effect was so pronounced that the measurement results were significantly influenced by artefacts arising from strong beam distortion causing self-diffraction rings (see Supporting Figure S1) and even photo-induced damage. Notably, for pure PDMS, we could observe thermal effects only for higher pulse energies above 7.4 μJ. Thermal effects caused by absorption are a well-known phenomenon in NB, with several opportunities for efficient mitigation [42]. Therefore, we have reduced the pulse energies in our measurements on PDMS/NB down to 0.8 μJ and also lowered the repetition rate from 50 Hz to 10 Hz, aiming to mitigate thermal effects. However, up to a pulse energy of 0.8 μJ, we have not observed any nonlinear behaviour of the PDMS/NB samples. For higher pulse energies, we only observed thermal effects in combination with photo-induced damage caused by (non) linear absorption. Hence, it seems that the detection limit for the Kerr effect is above the damage threshold of the PDMS/NB samples. Notably, both individual materials do not show thermal effects at 1.2 μJ pulse energy. Thus, the thermal effects in PDMS/NB cannot be explained with a superposition of the individual material properties.
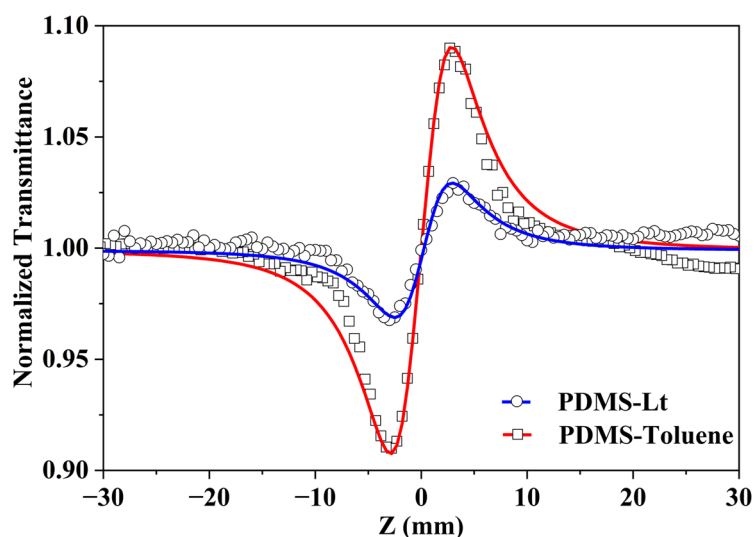


**Figure 4.** The comparative CA Z-scan profiles of the PDMS incorporated with 2,6-lutidine and toluene at a pulse energy of 5.4 μJ. Symbols are the experimental data and solid lines indicate the theoretical fit.

In addition to the inherent NLO properties and swelling behaviour, we can, therefore, identify a third pivotal factor for material selection: the absorption properties. Besides possible thermal nonlinearities or degradation of the material, one has to keep in mind other potential limitations for the design of photonic devices arising from absorption. As mentioned earlier, it is common practice to compensate for a relatively low NLO effect in materials by increasing the light–matter interaction length, thus achieving the same phase-shift of a wave passing through the material. For this argument to remain valid, it is, of course, necessary to assume a sufficiently low material absorption, ensuring low absorption losses on the desired interaction length. At a 532 nm wavelength, which was used in this study, the linear absorption coefficient for NB is around $\alpha = 2 \text{ m}^{-1}$, but only $\alpha = 0.24 \text{ m}^{-1}$ for TL [43,44].

At 400 nm wavelength, the disparity in linear absorption becomes even more pronounced, showing a 30-fold difference between NB and TL, with an increasing trend for shorter wavelengths. This tendency suggests a distinct advantage of the PDMS/TL composite material across short wavelength applications in the ultraviolet (UV) regime. For NB, one of the most well-known NLO materials, the composite material PDMS/NB not only showed the highest thermal contributions but also exhibited the lowest swelling effect in PDMS.

To exclude any remaining thermal contributions to the nonlinear properties of the PDMS/TL and PDMS/LT samples, intensity-dependent CA Z-scan measurements have been performed. Figure 5 shows the CA Z-scan profiles of the samples illuminated with varying pulse energy. The measured profiles were again fit using Equation (1) (see solid lines in Figure 5), and the corresponding nonlinear refractive indices were derived. In both cases, the corresponding nonlinear refractive index stays constant over the irradiance (see insets in Figure 5). It is thus evident that the observed nonlinear refraction originates from the optical Kerr effect, and the thermal contributions can be neglected.
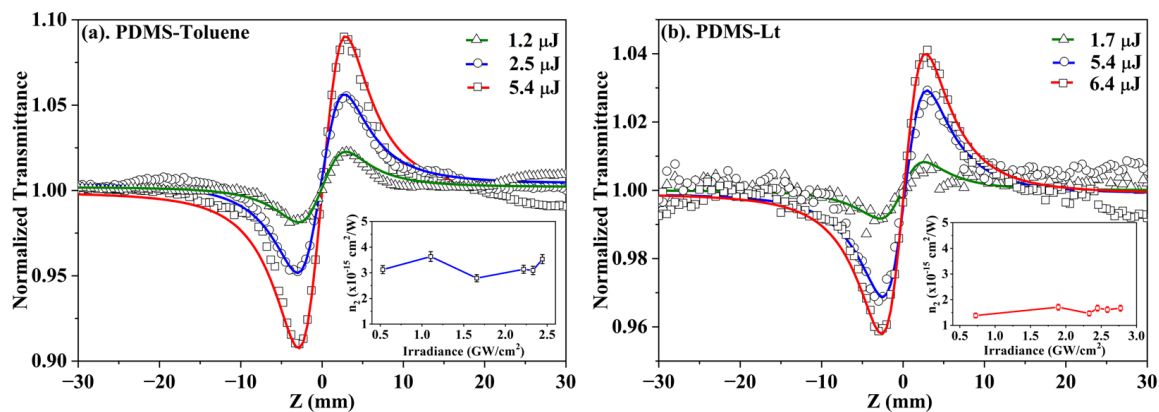


**Figure 5.** Energy-dependent CA Z-scan profiles of the PDMS-toluene and PDMS/Lt samples. Symbols represent the experimental data and solid lines show the theoretical fit. The insets show the nonlinear refractive indices as functions of the irradiance. An irradiance of 0.53 GW/cm$^2$ corresponded to a pulse energy of 1.2 µJ in our experiment.

The third-order nonlinear refractive indices of all composite samples are derived using Equation (1) and listed in Table 1. The nonlinear refractive index $n_2$ for PDMS-TL and PDMS-LT are 7 and 15 times smaller compared to pure NB, respectively.

**Table 1.** Nonlinear coefficients of the investigated samples derived from the data fitting.

| Sample | $n_2$ ($\times 10^{-15}$ cm$^2$/W) | $\beta_{2PA}$ (cm/GW) | Re($\chi^{(3)}$) ($\times 10^{-16}$ cm$^2$/V$^2$) |
|---|---|---|---|
| NB | 22.8 | 0.36 | 1.97 |
| LT | 7.1 | - | 0.56 |
| TL | 7.1 | - | 0.57 |
| PDMS/TL | 3.1 | - | 0.26 |
| PDMS/LT | 1.5 | - | 0.11 |
| PDMS/NB | n.a. * | n.a. * | n.a. * |

* Not applicable (n.a.) because of measurement results governed by significant artefacts caused by thermal effects and photo-induced damage within the entire experimental parameter range.

To further verify the origin of the nonlinearity, we have performed optical experiments on pure PDMS under uniaxial strain. In these experiments, we could only observe birefringence of the linear refractive index. In the z-scan measurements, we could not observe Kerr nonlinearity in pure PDMS with and without mechanical strain. We, therefore, conclude that the Kerr nonlinearity measured in our composite materials is not caused by strain, which is induced by the isotropic expansion of the PDMS due to swelling. Firstly, long-time stability tests have shown that the samples are stable up to certain photo-induced damage threshold, which is governed by the irradiance and the repetition rate of the laser (for details see Supporting Information).

## 4. Discussion

We have demonstrated a method for introducing optical Kerr nonlinearity to PDMS by utilizing the swelling of PDMS upon contact with various organic solvents. Investigating solvent swelling in PDMS reveals varying effects, with NB inducing the least and TL the most substantial swelling. These results emphasize that the material selection for our composite materials involves not only intrinsic NLO effects but also considerations regarding their distinct swelling behaviour. The swelling of polymers refers to an increase in the volume or size of a polymer when it comes into contact with a solvent or other liquids. The process of swelling involves the penetration of solvent molecules into a polymer host-matrix, causing the polymer chains to separate and the material to expand. The Flory–Rehner theory is a theoretical model that describes the swelling of polymers in a solvent. Parameters that determine the swelling behaviour of a certain polymer/solvent combination include the interaction parameter, the elasticity of the polymer, and the statistics (e.g., chain lengths and orientation) of the polymer matrix [45].

The characterization of the composite materials using the Z-scan technique demonstrates the general feasibility of introducing Kerr nonlinearity to PDMS. The resulting composite materials exhibit solid film characteristics, allowing for further processing in planar optical waveguide geometries. Hence, unlike liquid films, there is no need for spacers to maintain film thickness. Surprisingly, despite the strong nonlinearity, NB proves less feasible for PDMS integration due to increased thermal effects and photo-induced damage. It is remarkable that these effects cannot be explained through a simple superposition of the properties of the two materials. The ability of PDMS/NB to handle the thermal impact is far lower compared to the individual materials, which renders PDMS/NB practically unsuitable for high-power photonic applications. A comparison between PDMS/TL and PDMS/LT demonstrates superior nonlinear properties in PDMS/TL, due to the larger swelling effect of TL along with its high transparency, especially for short wavelengths. The transparency of TL further allows for the utilization of its nonlinearity over large interaction lengths, thereby enhancing the nonlinear effect on the passing light wave.

## 5. Conclusions

In summary, we have introduced a facile method for fabricating cost-effective and scalable nonlinear optical composite materials, marked by a substantial nonlinear optical effect along with high transparency. Our findings reveal that optical nonlinearity can be introduced to PDMS through solvent swelling, and the NLO properties of the resulting composite materials exhibit a linear dependence on the incorporated amount of solvent. We additionally compare three distinct solvents as well as the resulting PDMS/solvent composite materials concerning their nonlinear optical (NLO) properties and assess their suitability in optical applications, considering various factors such as transparency and photo-stability. In particular, the PDMS/TL composite material has proven itself as a promising candidate with a nonlinear refractive index of $n_2 = 3.1 \times 10^{-15}$ cm$^2$/W and a nonlinear susceptibility of $\chi^{(3)} = 0.26 \times 10^{-16}$ cm$^2$/V$^2$. From an application standpoint, it is noteworthy that, in comparison to Nitrobenzene (NB), Toluene (TL), and 2,6-lutidine (LT), they are considered less harmful as they are nontoxic. However, they still necessitate encapsulation to prevent degassing and ensure long-term stability. We anticipate these results to open up new possibilities for the implementation of nonlinear photonic systems, especially on large areas in the future.

**Supplementary Materials:** The following supporting information can be downloaded at: https://www.mdpi.com/article/10.3390/opt5010005/s1, Figure S1: Closed aperture Z-scan profiles of PDMS/NB under various experimental conditions. (A–C): CA Z-scan profiles of PDMS/NB at 10 Hz repetition rate and a pulse energy of 0.8 µJ (A), 1.2 µJ (B), and 5 µJ (C); (D): Closed aperture Z-scan profiles of PDMS/NB at a repetition rate of 50 Hz and a pulse energy of 5.6 µJ; Figure S2: Long-time stability investigations. (a) transmittance of PDMS/TL under intense laser illumination; (b) comparative

z-scan profiles after different illumination durations at a repetition rate of 50 Hz; (c) z-scan profile after the laser-induced damage threshold has been reached.

## References

1. Wang, Y.; Lin, C.-Y.; Nikolaenko, A.; Raghunathan, V.; Potma, E.O. Four-wave mixing microscopy of nanostructures. *Adv. Opt. Photon.* **2011**, *3*, 1–52. [CrossRef]
2. Boyd, R.W. *Nonlinear Optics*; Academic Press, Inc.: Cambridge, MA, USA, 2008.
3. Zhang, Y.; Lu, D.; Yu, H.; Zhang, H. Low-Dimensional Saturable Absorbers in the Visible Spectral Region. *Adv. Opt. Mater.* **2019**, *7*, 1800886. [CrossRef]
4. Schneider, T. *Nonlinear Optics in Telecommunications*; Springer Science & Business Media: Dordrecht, The Netherlands, 2004.
5. Garmire, E. Nonlinear optics in daily life. *Opt. Express* **2013**, *21*, 30532. [CrossRef]
6. Zhang, M.; Buscaino, B.; Wang, C.; Shams-Ansari, A.; Reimer, C.; Zhu, R.; Kahn, J.M.; Lončar, M. Broadband electro-optic frequency comb generation in a lithium niobate microring resonator. *Nature* **2019**, *568*, 373–377. [CrossRef]
7. Li, M.; Chang, L.; Wu, L.; Staffa, J.; Ling, J.; Javid, U.A.; Xue, S.; He, Y.; Lopez-Rios, R.; Morin, T.J.; et al. Integrated Pockels laser. *Nat. Commun.* **2022**, *13*, 5344. [CrossRef]
8. Haag, H.; Hönerlage, B.; Briot, O.; Aulombard, R.L. Influence of defect states on the nonlinear optical properties of GaN. *Phys. Rev. B* **1999**, *60*, 11624–11630. [CrossRef]
9. Zhou, S.; Liu, X.; Yan, H.; Chen, Z.; Liu, Y.; Liu, S. Highly efficient GaN-based high-power flip-chip light-emitting diodes. *Opt. Express* **2019**, *27*, A669–A692. [CrossRef]
10. Zhou, S.; Liu, X.; Yan, H.; Gao, Y.; Xu, H.; Zhao, J.; Liu, S. The effect of nanometre-scale V-pits on electronic and optical properties and efficiency droop of GaN-based green light-emitting diodes. *Sci. Rep.* **2018**, *8*, 11053. [CrossRef]
11. Xia, P.; Kim, C.; Lu, F.; Kanai, T.; Akiyama, H.; Itatani, J.; Ishii, N. Nonlinear propagation effects in high harmonic generation in reflection and transmission from gallium arsenide. *Opt. Express* **2018**, *26*, 29393–29400. [CrossRef]
12. Dalton, L.R.; Günter, P.; Jazbinsek, M. . *Organic Electro-Optics and Photonics: Molecules, Polymers, and Crystals*; Materials Research Society and Cambridge University Press: Cambridge, UK, 2015.
13. Xu, J.; Li, X.; Xiong, J.; Yuan, C.; Semin, S.; Rasing, T.; Bu, X.H. Halide Perovskites for Nonlinear Optics. *Adv. Mater.* **2020**, *32*, 1806736. [CrossRef]
14. Guo, B.; Xiao, Q.; Wang, S.; Zhang, H. 2D Layered Materials: Synthesis, Nonlinear Optical Properties, and Device Applications. *Laser Photon. Rev.* **2019**, *13*, 1800327. [CrossRef]
15. You, J.; Bongu, S.; Bao, Q.; Panoiu, N. Nonlinear optical properties and applications of 2D materials: Theoretical and experimental aspects. *Nanophotonics* **2018**, *8*, 63–97. [CrossRef]
16. Mistark, P.A.; Park, S.; Yalcin, S.E.; Lee, D.H.; Yavuzcetin, O.; Tuominen, M.T.; Russell, T.P.; Achermann, M. Block-Copolymer-Based Plasmonic Nanostructures. *ACS Nano* **2009**, *3*, 3987–3992. [CrossRef]
17. Alvarez-Fernandez, A.; Cummins, C.; Saba, M.; Steiner, U.; Fleury, G.; Ponsinet, V.; Guldin, S. Block Copolymer Directed Metamaterials and Metasurfaces for Novel Optical Devices. *Adv. Opt. Mater.* **2021**, *9*, 2100175. [CrossRef]
18. Piechulla, P.M.; Muehlenbein, L.; Wehrspohn, R.B.; Nanz, S.; Abass, A.; Rockstuhl, C.; Sprafke, A. Fabrication of Nearly-Hyperuniform Substrates by Tailored Disorder for Photonic Applications. *Adv. Opt. Mater.* **2018**, *6*, 1701272. [CrossRef]
19. Haynes, C.L.; Van Duyne, R.P. Nanosphere Lithography: A Versatile Nanofabrication Tool for Studies of Size-Dependent Nanoparticle Optics. *J. Phys. Chem. B* **2001**, *105*, 5599–5611. [CrossRef]
20. Shutsko, I.; Buchmüller, M.; Meudt, M.; Görrn, P. Plasmon-Induced Disorder Engineering for Robust Optical Sensors. *Adv. Opt. Mater.* **2022**, *10*, 2102783. [CrossRef]
21. Buchmüller, M.; Shutsko, I.; Schumacher, S.O.; Görrn, P. Harnessing Short-Range Surface Plasmons in Planar Silver Films via Disorder-Engineered Metasurfaces. *ACS Appl. Opt. Mater.* **2023**, *1*, 1777–1782. [CrossRef]
22. Wang, B.; Yu, P.; Wang, W.; Zhang, X.; Kuo, H.C.; Xu, H.; Wang, Z.M. High-Q Plasmonic Resonances: Fundamentals and Applications. *Adv. Opt. Mater.* **2021**, *9*, 2001520. [CrossRef]

23. Wang, B.; Yu, P.; Wang, W.; Zhang, X.; Kuo, H.; Xu, H.; Wang, Z.M. Theoretical Description of Node-Aligned Resonant Waveguide Gratings. *Optics* **2022**, *3*, 60–69.

24. Henkel, A.; Schumacher, S.O.; Meudt, M.; Knoth, C.; Buchmüller, M.; Görrn, P. High-Contrast Switching of Light Enabled by Zero Diffraction. *Adv. Photonics Res.* **2023**, *4*, 2300230. [CrossRef]

25. Nalwa, H.S. Organic Materials for Third-Order Nonlinear Optics. *Adv. Mater.* **1993**, *5*, 341–358. [CrossRef]

26. González-Estefan, J.H.; Gonidec, M.; Vu, T.T.; Daro, N.; Chastanet, G. In Situ Fine-Tuning of Microfluidic Chips by Swelling and Its Application to Droplet Microfluidics. *Adv. Mater. Technol.* **2019**, *4*, 1900232. [CrossRef]

27. Dangla, R.; Gallaire, F.; Baroud, C.N. Microchannel deformations due to solvent-induced PDMS swelling. *Lab Chip* **2010**, *10*, 2972–2978. [CrossRef]

28. Qi, D.; Zhang, K.; Tian, G.; Jiang, B.; Huang, Y. Stretchable Electronics Based on PDMS Substrates. *Adv. Mater.* **2021**, *33*, 2003155. [CrossRef]

29. Polywka, A.; Jakob, T.; Stegers, L.; Riedl, T.; Görrn, P. Facile Preparation of High-Performance Elastically Stretchable Interconnects. *Adv. Mater.* **2015**, *27*, 3755–3759. [CrossRef]

30. Kolaric, B.; Desprez, S.; Brau, F.; Damman, P. Design of curved photonic crystal using swelling induced instabilities. *J. Mater. Chem.* **2012**, *22*, 16205–16208. [CrossRef]

31. Usui, K.; Matsumoto, K.; Katayama, E.; Akamatsu, N.; Shishido, A. A Deformable Low-Threshold Optical Limiter with Oligothiophene-Doped Liquid Crystals. *ACS Appl. Mater. Interfaces* **2021**, *13*, 23049–23056. [CrossRef] [PubMed]

32. Haripadmam, P.C.; Thanuja, T.H.; Varsha, G.S.; Beryl, C.D.; Aji, A. Nonlinear optical absorption in PVA films doped by the novel natural dye extract from *C. redflash* leaves. *Opt. Mater.* **2021**, *112*, 110804. [CrossRef]

33. Fu, B.; Sun, J.; Cheng, Y.; Ouyang, H.; Compagnini, G.; Yin, P.; Zhang, H. Recent Progress on Metal-Based Nanomaterials: Fabrications, Optical Properties, and Applications in Ultrafast Photonics. *Adv. Funct. Mater.* **2021**, *31*, 2107363. [CrossRef]

34. Kauranen, M.; Zayats, A.V. Nonlinear plasmonics. *Nat. Photonics* **2012**, *6*, 737–748. [CrossRef]

35. Bai, T.; Dong, N.; Cheng, H.; Cheng, Q.; Wang, J.; Chen, Y. $CH_3NH_3PbI_3$ perovskite:poly(N-vinylcarbazole) blends for broadband optical limiting. *RSC Adv.* **2017**, *7*, 1809–1813. [CrossRef]

36. Johnson, V.; Gandhiraj, V. Enhanced nonlinear characteristics of polymer-perovskite hybrid ($PVA/CMC/LaAlO_3$) fabricated via solution casting process for optical limiting applications. *J. Mater. Sci. Mater. Electron.* **2023**, *34*, 2103. [CrossRef]

37. Guo, J.; Shi, R.; Wang, R.; Wang, Y.; Zhang, F.; Wang, C.; Chen, H.; Ma, C.; Wang, Z.; Ge, Y.; et al. Graphdiyne-Polymer Nanocomposite as a Broadband and Robust Saturable Absorber for Ultrafast Photonics. *Laser Photon. Rev.* **2020**, *14*, 1900367. [CrossRef]

38. Mu, H.; Lin, S.; Wang, Z.; Xiao, S.; Li, P.; Chen, Y.; Zhang, H.; Bao, H.; Lau, S.P.; Pan, C.; et al. Black Phosphorus–Polymer Composites for Pulsed Lasers. *Adv. Opt. Mater.* **2015**, *3*, 1447–1453. [CrossRef]

39. Lee, J.N.; Park, C.; Whitesides, G.M. Solvent Compatibility of Poly(dimethylsiloxane)-Based Microfluidic Devices. *Anal. Chem.* **2003**, *75*, 6544–6554. [CrossRef] [PubMed]

40. Sheik-Bahae, M.; Said, A.A.; Van Stryland, E.W. High-sensitivity, single-beam n_2 measurements. *Opt. Lett.* **1989**, *14*, 955. [CrossRef]

41. Sheik-Bahae, M.; Said, A.; Wei, T.-H.; Hagan, D.; Van Stryland, E. Sensitive Measurement of Optical Nonlinearities Using a Single Beam. *IEEE J. Quantum Electron.* **1990**, *26*, 760–769. [CrossRef]

42. Bongu, S.R.; Buchmüller, M.; Neumaier, D.; Görrn, P. Electric Control of Thermal Contributions to the Nonlinear Optical Properties of Nitrobenzene. *Adv. Phys. Res.* **2023**, *3*, 2300053. [CrossRef]

43. Cabrera, M.H.; Marcano, O.A.; Ojeda, A.J.; Wetter, N.U.; Frejlich, J. Absorption Spectra of Nitrobenzene Measured with Incoherent White-Light Excitation. *AIP Conf. Proc.* **2008**, *992*, 1183–1188.

44. Kedenburg, S.; Vieweg, M.; Gissibl, T.; Giessen, H. Linear refractive index and absorption measurements of nonlinear optical liquids in the visible and near-infrared spectral region. *Opt. Mater. Express* **2012**, *2*, 1588–1611. [CrossRef]

45. Flory, P.J.; Rehner, J., Jr. Statistical mechanics of cross-linked polymer networks II. Swelling. *J. Chem. Phys.* **1943**, *11*, 521–526. [CrossRef]